

Investigation impact of stressed state conditions and thermomechanical parameters on the texture and structure evolution in 1565ph aluminium alloy

V V Yashin¹, E V Aryshensky², R F Kawalla³, V N Serebryany⁴ and S V Rushchits⁵

¹ZAO Alcoa SMZ, 29, Alma-Atinskaya str., Samara, 443051, Russia

²Samara State Aerospace University, 45, Moskovskoye Shosse, Samara, 443086, Russia

³Technische Universität Bergakademie Freiberg, Bernhard-v.-Cotta-Str. 4, 09599 Freiberg, Germany

⁴A.A.Baikov Institute of Metallurgy and Material Science RAS 49, Leninskiy prospect Moscow, 119991, Russia

⁵South Ural State University, 76, Lenin prospect, Chelyabinsk, Russia

E-mail: vasily.yashin@alcoa.com

Abstract. The paper is devoted to study of the impact stress condition and thermomechanical treatment parameters on the structure and texture evolution of new 1565 ph aluminum alloy. For that purposes, we use test on Gleeble equipment, FM calculation, optical microscopy and x ray diffraction texture analysis. The dependency between the deformation texture components development and strain rate value was established. Differences in the texture evolution at uniaxial compression stress and plain strain mode were revealed.

1. Introduction

Despite of the new types of materials emergence, aluminum alloys still maintain their competitiveness and remain much in demand, especially, in aerospace industry. Aluminum alloys are so attractable because of combination low weight with high formability and acceptable strength [1]. That is why new alloys development and existing aluminum alloys improvement is continuously ongoing. Zirconium or scandium addition to aluminum alloys have become one of the key practices of its creation over the recent 10 – 15 years [1 - 3]. Its representative is 1565ph alloy (Al-Mg-Zn-Zr), recently developed by the Russian scientists [2]. This alloy is designed for low temperature applications, i.e. for aerospace field, cryogenic liquids transportation and the extreme north environment; it also demonstrates high strength and good weldability.

However, properties get in laboratory condition cannot be automatically achieved during real industrial process. It is well known that in order to obtain necessary properties level, one should control the texture and structure evolution and other important parameters like temperature and mechanical behavior during all manufacturing process [4 - 8]. Investigation of mechanical properties evolution was performed for this alloy in [9,10]. The texture evolution during hot rolling in the continuous mill was studied in [10]. However, we still need to establish impact of main technology parameters as well as stressed state condition on the texture evolution during thermomechanical treatment. It allows us to create reliable models and get possibility to achieve the required texture and structure in any combination of technological conditions.

In the present paper, the texture and structure evolution for two different type of stress condition and wide range of temperature and strain rate values is studied. Two different with different stress condition

2. Experimental procedure



All deformations are carried out on plane-strain and axial compression modes. Temperature and strain rate parameters for each mode are presented in the Table 1, in all cases true strain did not exceed 1. The specimens had the following dimensions: for the plane strain: $h = 10$ mm, $w = 26$ mm and $l = 28$ mm, and for axial compression: $h = 15$ mm, $d = 10$ mm. The samples were collected after the hot rolling in industrial reversing mill and had fully recrystallized structure [10].

Table 1. Temperature strain rate parameters for two different stress condition.

Plane strain mode								
Temperature, °C	350	400		440			490	
Strain rate ($\dot{\epsilon}$), s ⁻¹	10	10	1	10	50	0,1	1	10 90
Axial mode								
Temperature, °C	350	400		450			490	
Strain rate ($\dot{\epsilon}$), s ⁻¹	50	50	0,1	1	10	50	50	

After the deformation, the samples were quenched in water for texture and structure fixation. Then for the further X-ray structural analysis specimen was cut out from the middle section. Some specimens were cut crosswise for microstructure analysis in polarized light in Axiovert-40MAT microscope.

The texture, represented by four incomplete pole figures (PF) {111}, {200}, {220} and {311}, was analyzed by „reflection“ method in $C_{\alpha}K_{\alpha}$ -radiation, using x-ray diffractometer DRON-7. Pole figures view plane was parallel to the rolling direction. The following angle ranges were applied: inclination $\alpha = 0-70^\circ$ and rotation $\beta = 0-360^\circ$ with 5° step. The defocusing-induced decrease in the intensity at the periphery of a PF was corrected using coefficients calculated for PF recording conditions [11]. The orientation distribution function (ODF) and the volume fractions of the main orientations were calculated using the method of approximation by a large number (2000) of Gaussian normal distributions. For convenience of orientations distribution, function application three-dimensional function may be approximately represented by a sum of standard functions (texture components, perfect orientations dispersion); the combination of these texture components was selected based on analyses of sections of orientations distribution function, computed based on experimental pole figures. Newly created orientations file with three Euler angles and preliminary functions parameters, was processed by Texxor [12].

We also analyzed the stress components distribution and the accumulated strain field into workpiece for both deformation modes. For its calculation we use the DEFORM Software. The computation was performed for all possible process regimes presented in Table 1.

3. Experimental results

Results of microstructural analysis for different combinations of strain rates and temperature entities are shown in Figure 1.

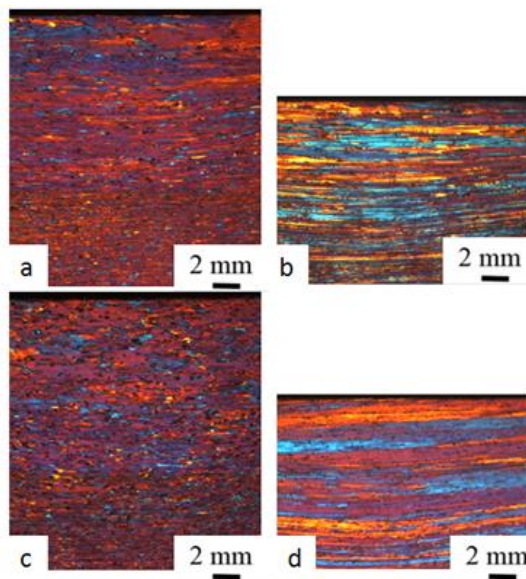


Figure 1. Comparison of microstructure analysis results: top part of cross section
 (a) axial compression ($T = 450\text{ }^{\circ}\text{C}$, $\dot{\epsilon} = 10\text{ s}^{-1}$); (b) plain strain mode ($T = 440\text{ }^{\circ}\text{C}$, $\dot{\epsilon} = 10\text{ s}^{-1}$);
 (c) axial compression ($T = 440\text{ }^{\circ}\text{C}$, $\dot{\epsilon} = 50\text{ s}^{-1}$); (d) plane strain mode ($T = 440\text{ }^{\circ}\text{C}$, $\dot{\epsilon} = 50\text{ s}^{-1}$).

It should be noted that we show results mainly for regimes with high strain rates, as they present the interest for development thermomechanical processes with large deformation speed. Significant difference in structure (Figure 1) is observed for two types of stressed state. Elongated deformed grains are clearly seen in the entire specimen sections in the case of plane strain. In the case of axial compression, the structure has mixed nature with recrystallized grain close to the near-surface zone and deformed macrostructure in the specimen mid-section. Such difference is explained by the presence of large sticking friction zone in cylindrical specimen. That zone is clearly seen in Figure 2, which shows accumulated strain distribution into workpiece for axial compression mode.

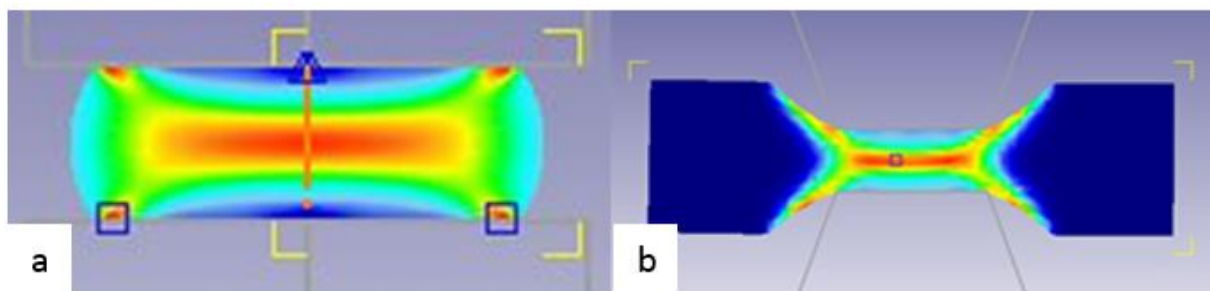


Figure 2. Accumulated strain distribution for different stress conditions, which was calculated in DEFORM: (a) axial compression ($T = 450\text{ }^{\circ}\text{C}$, $\dot{\epsilon} = 10\text{ s}^{-1}$); (b) plane strain condition ($T = 440\text{ }^{\circ}\text{C}$, $\dot{\epsilon} = 10\text{ s}^{-1}$)

As seen from Figure 2 a, in near-surface zone workpiece actually doesn't get any deformation. As a result, this zone almost fully corresponds to the area with recrystallized grain in real cylindrical workpiece. Actually, these grains don't get any deformation during axial compression and save from hot rolling process. In the opposite way, in the case of plane strain condition the accumulative strain is more uniformly distributed across the workpiece section. The different in accumulative strain distribution, explains the distinction in the observed microstructure. It should be noted, that the strain rate increasing

in this investigation conditions has almost no effect on microstructure evolution in both deformation modes.

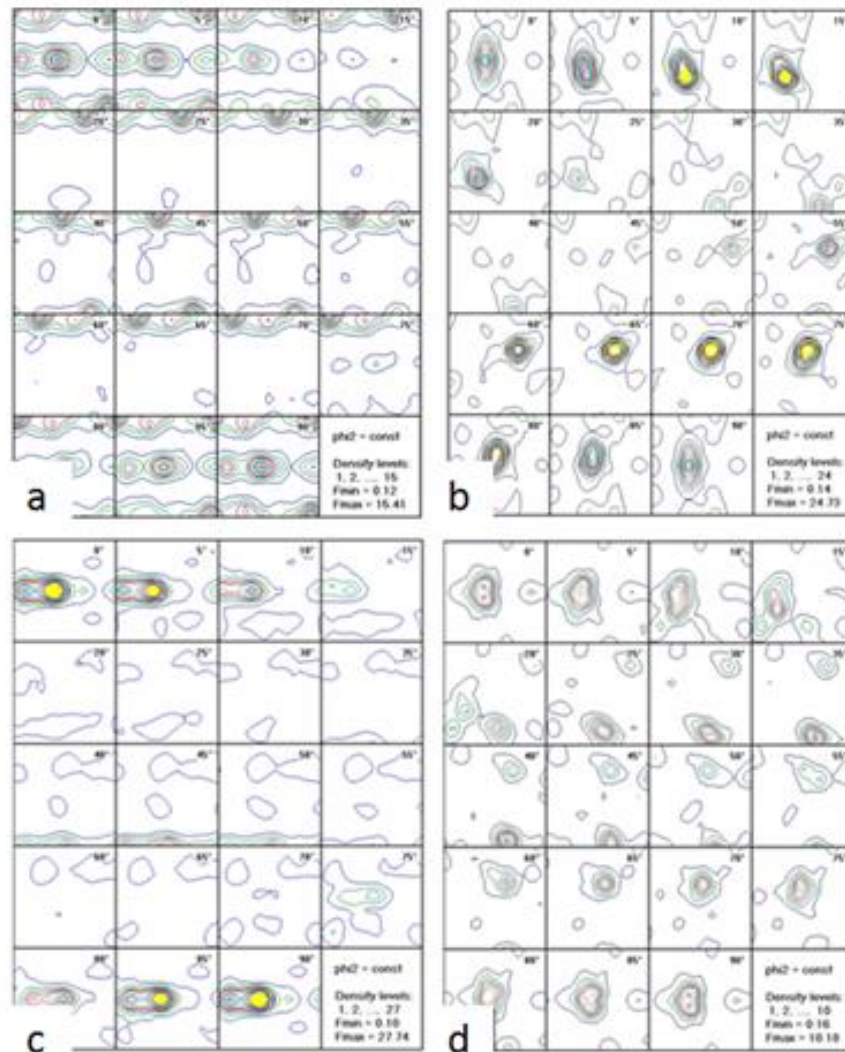


Figure 3. Comparison of the X-ray texture analyzes results:

- (a) Axial compression ($T = 450\text{ }^{\circ}\text{C}$, $\dot{\epsilon} = 1\text{ s}^{-1}$); (b) Plane strain condition ($T = 450\text{ }^{\circ}\text{C}$, $\dot{\epsilon} = 1\text{ s}^{-1}$);
 (c) Axial compression ($T = 450\text{ }^{\circ}\text{C}$, $\dot{\epsilon} = 10\text{ s}^{-1}$); (d) Plane strain condition ($T = 440\text{ }^{\circ}\text{C}$, $\dot{\epsilon} = 10\text{ s}^{-1}$).

Comparison between texture analysis results for axial compression and plane strain condition are illustrated in Figure 3 a, b. In the first case we have mixed texture, including both cube and deformation components. In the second case, mostly deformation texture components are observed. In plane strain condition in some areas of Euler space the deformation texture is strongly pronounced, however, in general, its volume is not very large.

Comparison of the texture analysis results (Figure 3 c, d) for higher strain rates demonstrates that clearly pronounced deformation texture are observed in axial compression case. In case of the plane strain condition the deformation texture is not so pronounced, however it could be observed in more Euler space areas than after axial compression.

The differences in the texture components can be easily explained by distinction in stressed state conditions (Figure 4), which have significant effect on their evolution.

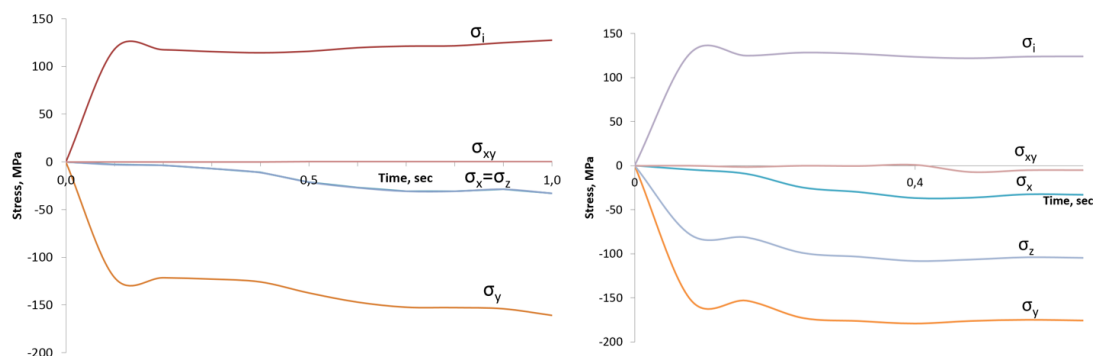


Figure 4. Stress distribution in the samples middle section: (a) axial compression (b) plain strain condition.

In conclusion, the strain rate influence on deformation components growth is investigated (Figure 5).

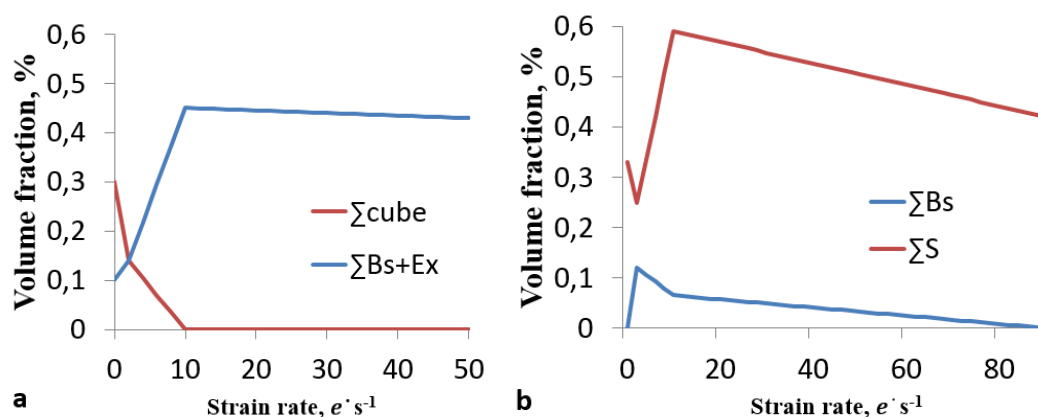


Figure 5. The texture component dependence on strain rates: (a) for axial compression; (b) for plane strain condition.

The similar picture is observed in both cases. The strain rate impact on texture evolution drastically increase, in the range of 0 to 10 s⁻¹. Then its, reaches peak and start decreasing: slowly in case of axial compression and more fast in plane strain condition. We can also conclude from Figure 3 a, b, analyze that logarithmic strain about 1 is no enough for full transformation of the cube texture components into deformation texture in case of low strain rate entities. These are significant results, which support the necessity of the high-speed hardening [13 – 14] consideration in the texture evolution models for such type of alloys.

4. Summary

1) The alloy 1565ph demonstrates the absence of bending to recrystallization. However, in axial compression mode not only deformed, but also recrystallized structure is observed. Simulation in DEFORM software show, that the main reason for such type of structure is the presents of sticking friction zone. Grain in this zone actually do not change during deformation process.

2) Distinction between main texture components, which are observed in different treatment modes, could be explain by various stress condition. Strain rate with combination in stress also has significant effect on the texture evolution, as result this influence must be accounted in mathematical model of texture evolution for such group of alloys in two different test mode.

Reference

- [1] Davydov V G, Elagin V I, Zakharov V V and Rostova T D 1996 Alloying aluminium alloys with scandium and zirconium additives *J. Metal Science and Heat Treatment* **38 VII-VIII** 347-352
- [2] Oryshenko A S, Osokin E P, Barakhtina N N, Drits A M and Sosedkov S M 2012 Aluminum – magnesium alloy 1565 for cryogenic application *J. Tsvetnye Metally* **11** 84-90
- [3] Røyset J and Ryum N 2005 Scandium in aluminium alloys *International Materials Reviews* **50 I** 19-44
- [4] Gorelova S, Schaeben H and Kawalla R. 2014 Quantifying texture evolution during hot rolling of magnesium twin roll cast strip *Materials Science and Engineering A* **602** 134-142
- [5] Hirsch J 2005 Texture evolution and earing in aluminium can sheet *Materials Science Forum* **495-497 II** 1565-157
- [6] Aryshenskii E V, Aryshenskii V Y, Grechnikova A F and Beglov E D 2014 Evolution of Texture and Microstructure in the Production of Sheets and Ribbons from Aluminum Alloy 5182 in Modern Rolling Facilities *Metal Science and Heat Treatment* **56 VII-VIII** 347-352
- [7] Nam A, Prüfert U, Eiermann M and Kawalla R 2016 Modelling the temperature evolution during hot reversing strip rolling of magnesium alloys *Materials Science Forum* **854** 140-145
- [8] Kawalla R, Graf M and Tokmakov K 2010 Simulation system of multistage hot rolling process of flat Products *J. Metalurgija* **49-III** 175-179
- [9] Rushchits S, Aryshenskii E, Kawalla R and Serebryany V 2016 Investigation of texture structure and mechanical properties evolution during hot deformation of 1565 aluminum alloy *Materials Science Forum* **854** 73-78
- [10] Rushchits S V, Aryshensky E V, Sosedkov S M and Akhmed'Yanov A.M. 2016 Modeling the hot deformation behavior of 1565ch aluminum alloy *Key Engineering Materials* **684** 35-41
- [11] Serebryany V N, Kurtasov S F and Litvinovich M A 2007, Analysis of ODF errors upon the reversion of polar figures with the use of the statistical method of ridge estimations, *Zavod. Lab., Diagn. Mater.* **73 IV** 29– 35
- [12] Kurtasov S F 2007, Quantitative analysis of the rolling textures of materials with a cubic symmetry of crystal lattice, *Zavod. Lab., Diagn. Mater.* **73 VII** 29–35
- [13] Asaro R J 1983 Micromechanics of Crystals and Polycrystals *Advances in Applied Mechanics* **23** 1-115.
- [14] Beaudoin A J, Mathur K K, Dawson P R, Kocks U F 1995, *J. Plast.* **11** 501-521